Study of the Friction Stir Welding For A516 Low Carbon Steel

Prof. Dr. Qasim Mouhamed Doos
Department of Mechanical Engineering
College of Engineering - Baghdad University
E- mail : Kasim_daws@yahoo.com

Riyadh F. Farhan
Department of Mechanical Engineering
College of Engineering - Baghdad University
E-mail: riadh_engineer81@yahoo.com

ABSTRACT

The main objective of present work is to describe the feasibility of friction stir welding (FSW) for joining of low carbon steel with dimensions (3 mm X 80 mm X 150 mm). A matrix (3×3) of welding parameters (welding speed and tool rotational speed) was used to see influence of each parameter on properties of welded joint .Series of (FSW) experiments were conducted using CNC milling machine utilizing the wide range of rotational speed and transverse speed of the machine. Effect of welding parameters on mechanical properties of weld joints were investigated using different mechanical tests including (tensile and microhardness tests). Micro structural change during (FSW) process was studied and different welding zones were investigated using optical microscope. The stir welding experiments conducted that show the low carbon steel can be welded using (FSW) process with maximum welding efficiency (100.02%) in terms of ultimate tensile strength using best result of welding parameters (700 RPM, 25 mm/min, tool rotational speed and welding speed respectively and 0.2 mm plunging depth of welding tool) ,there is afirst time that we obtain the efficiency reach to 100.02 % to weld this type of low carbon steel by FSW. The corrosion resistance was measure which is the new test on the welding by this way and we obtained different result from the result on traditional welding processes and the result that obtained show the corrosion resistance for this welding plate better than the base metal. Maximum temperature has been calculated numerically by using the ANSYS program. The obtained peak temperature is 1102°C, A percentage minimum of the melting point .

KEYWORDS : FSW**,** Mechanical properties, FEM simulation .

دراسة اللحام بالخلط الاحتكاكي للفولاذ الواطيء الكاربون A516

أ. د. قاسم محمد دوس
قسم الهندسة الميكانيكية
كلية الهندسة / جامعة بغداد

م.م. رياض فرع فرحان
قسم الهندسة الميكانيكية
كلية الهندسة / جامعة بغداد

الخلاصة

اللحام بالخلط الاحتكاكي هي احدى عمليات اللحام الحديثة ، اللحام بالخلط الاحتكاكي هي احدى طرق لحام الحالة الصلبة التي يتم بها دوران اداة الخلط وتجبر القطعتان على الترابط بتأثير مركب من الحرارة والجهد الميكانيكي . ان الغرض الرئيسي من هذا العمل هو لبيان امكانية طريقة اللحام بالخلط الاحتكاكي من ربط قطعتان من الفولاذ المنخفض الكربون ذات ابعاد (150 ملم ×80 ملم × 3 ملم) .تم استخدام مصفوفة (3×3) من متغيرات اللحام والتي تمثل(السرعة الدورانية لعدة اللحام والسرعة الخطية للحام) لدراسة تأثير كل متغير من هذه المتغيرات بشكل منفـــصل على خواص وصلات اللحام .تم القيام بسلسلة من تجارب اللحام باستعمال ماكنة تفريز الميكانيكي المبرمجــــة (CNC) ذات المدى الواسع من

السرع الدورانية والسرع الخطية لهذه الماكنة .تأثير متغيرات اللحام على الخواص الميكانيكية لوصلات اللحام تم دراستها بالأعتماد على الفحوصات الميكانيكية المختلفة (فحص الشد ، فحص الصلادة) . كما تم دراسة التغيرات الميتالورجية خلال عملية اللحام ودراسة مناطق اللحام المختلفة بأستعمال المجهر الضوئي . بناءا" على التجارب المختلفة في هذه الدراسة أتضح من النتائج بأن الفولاذ المنخفض الكربون قابل للحام بهذه الطريقة مع الحصول على اقصى كفائة لحام وصلت الى (100,2%) بدلالة مقاومة الشد بأستخدام متغيرات اللحام المثلى (700 دورة بالدقيقة سرعة دورانية ، 25 ملم / دقيقة سرعة لحام ، 0,2 ملم عمق عدة الغرز) تم حساب اقصى درجة حرارة عدديا"باستعمال برنامج ANSYS . وكانت اقصى درجة حرارة حصلنا عليها هي (1102 درجة سيليزية) التي كانت اقل بكثير من درجة حرارةانصهارالفولاذ الكاربوني

كلمات رئيسية : لحام بالخلط الاحتكاكي ، الخواص الميكانيكية ، المحاكاة باستخدام طريقة العناصر المتناهية

1 INTRODUCTION

Exploration for welding process is expanding , one of the welding process is (FSW) , It is a modern method to joint parts as a solid state welding process , anon consumable tool used . The tool have large diameter called shoulder and small diameter called pin . And by the friction between the piece and shoulder the heat will be generated.There is some of advantages in welding rejoin such as reduced of porosity ,lower distortion and shrinkage. (Thomas 1991).(Scott M. 2005) present tool geometry and process parameters for PCBN tool . (Thomas 1991) describe the tool and equipment required to study FSW .(Naiyi 2004)study the FSW of Mg alloy .(Takehito 2006) tried to joint dissimilar metal such as Al to steel. (Tery and 2003) focused on heat flow in FSW tool.(X.K.Zhn 2003) simulated temperature and stresses in FSW for stainless steel . ultrahigh carbon steel during FSW was applied by (Y.S. Sato 2007).(T. Saeid 2008) focused on the welding speed and it is effected on the properties of stir zone .

2 EXPERIMENTAL PROCEDURES

An overview of the used FSW tool is shown in figure 1 quantitative information can be illustrated in Table 1. The tool is fitted into a tool holder and linked to the machine spindle. The tool is rotated clockwise as seen from above the weld.
 (FSW) were produced on plates A516 low carbon steel (3 mm thick). The plates of Low Carbone Steel were prepared with the dimensions (160mmx80mmx3mm) as shown in figure 2 .Each

two plates were joining with the friction stir welding.
The plates were manufactured to get minimum faults which affect on the quality of welding.
Chemical analysis has been conducted in the Specialized Institute for Engineering Industries for these plates.
The table 2 shows the chemical composition for the Steel plate that used in present work.. Welds were made in the butt-joint configuration on samples typically.The dimensions 150 mm length and 80 mm width. The shoulder diameter used (16 mm), The length of the pin was approximately (2.6 mm). A Tungsten carbide (WC) tool was used. Table 2 gives the FSW parameters for low carbon steel. The Vickers microhardness of the weld have been measured in the center of the thicknessin the addvancing side. Tensile specimens were prepared accordance to ASTM E8.

3 RESULTS AND DISCUSSION
3.1 Fsw Joint
It is clearly seen that sound joints are obtained up to the welding speed of 50 mm/min. However, at a higher speed of 150 mm/min, a groove-like defect is observed in the joint advancing side figure 3. This defect can seriously degrade the mechanical properties of the weld metal. Previous studies revealed that groove-like defects are primarily formed when the heat input during FSW is insufficient. In this situation, the material could not easily flow to fill up the gap generated by the tool pin. As will be describedin subsequent section, one of the key parameters that have an essential influence on the heat input is the welding speed.

With increasing the welding speed, the heat input would be decreased gradually up to a limit that the generated frictional heat is insufficient to allow viscoplastic material flow and therefore, the groove-like defect is more likely to occur.

3.2 The Weld Thermal

  The temperature distribution varies in time and space; hence a three-dimensional, transient, isotropic solid with moving heat source model was used to simulate FSW thermal process. The conservation of energy in a differential form can be written as (ANSYS v.10),(John 2005).

$$\rho \, c_p(T) \frac{\partial T}{\partial t} = k(T) \left(\frac{\partial^2 T}{\partial x^2} + \frac{\partial^2 T}{\partial y^2} + \frac{\partial^2 T}{\partial z^2} \right) + \dot{Q} \quad (1)$$

Where: ρ : density
 $c_p(T)$: specific heat
T : temperature
 t is time
 k(T) : temperature

$\dot{Q}$ is rate of heat generation
Temperature dependent thermal properties. Three boundary conditions associated with equ. (1) as shown in figure (4). The first is the energy loss by heat convection which is defined by

$$Q_{conv} = h_c \left(T \, - T_a \right) \qquad (2)$$

Where:
Qconv: energy loss of by convection per unit area.
 hc: coefficient of the heat transfer (h=30 W/m2 °C
 T: absolute surface temperature.
Ta: absolute ambient temperature (Ta=298 °K).
The equivalent convection coefficient for the workpiece/backing plate interface is calculated by (Frigaard 2001),(Hwanga 2008)

$$Q_b = h_b \left(T \, - T_a \right) \qquad (3)$$

Where: Qb: energy loss of by convection per unit area.
hb: convection heat transfer coefficient. (h=350 W/m2 °C).

The third type is the radiation heat loss which is defined by

$$Q_{rad} = e \mathrm{F} \sigma_{SB} \left(T^4 - T_a^4 \right) \quad (4)$$

Where: Qrad: energy loss of by radiation per unit area.
 e: effective emissivity of radiant surface (e=0.5).
F: radiation view factors (F=1).
σSB: Stefan-Boltzman constant
(σSB =5.67×10-8 W/m2 °K4).
The heat generation during friction- stir is difficult. And in general we note that the total heat generated frome the shoulder may be used to compensate for deformation heat generation; this could be done by an adjusting coefficient of friction. Friction is a complex physical phenomenon that depends on parameters like material, surface roughness, lubrication, temperature and pressure Frictional heat generated by the shoulder face may be derived, where area element on shoulder face is:

$$dA = 2\,\pi\,\mathrm{r}\,\mathrm{dr} \qquad (5)$$

Frictional torque required is given by:

$$dM = \mu\,P\,r\,dA \;\; = 2\,\pi\,\mu\,P\,r^2\,dr \quad (6)$$

Where: M : torque
          μ is the friction coefficient
          P is the interfacial pressure
Frictional heat for the shaft rotating at rubbing angular speed of (1-δ)ω is:

$$dQ_s = (1 - \delta)\,\omega\,dM = 2\,\pi\,(1 - \delta)\,\omega\,\mu\,P\,r^2\,dr \quad (7)$$

where δ is the slip factor that compensate for tool/material relative velocity. Typical values for slip factor found in literature ranges between 0.6, 0.85 (Takehiko 2006). Total frictional heat of shoulder will be:

$$Q_s = \int_0^{R_s} dQ_s = \frac{2}{3}\pi\,(1-\delta)\,\omega\,\mu\,P\,R_s^3 \quad (8)$$

In similar concept, heat generated by lateral surface of the pin is :

$$Q_p = 2\,\pi\,(1-\delta)\,\omega\,\mu P\,L_p\,R_p^2 \quad (9)$$

Total frictional heat generated by the tool is the summation of equ. (9) and equ. (10) which is:

$$Q_T = 2\,\pi\,(1-\delta)\,\omega\mu\,P\left(\frac{R_s^3}{3}+L_p\,R_p^2\right) \quad (10)$$

During the process the tool travels at a constant speed (Vt). This motion was simulated by changing heat source location, as shown in Figure 5. according to the following equation:

Xi+1= Xi + Vt Δt   for   Li ≤ X ≤ Lw   (11)

Where Δt is the time required for the tool to travel from location Xi to Xi+1, (i.e. element size) and Vt is the tool traveling speed
Li : Welding Starting position = 2* Rs.
Lw: Weld length
.Final comments may be mentioned regarding ANSYS program description. The three dimensional element "*SOLID70*", shown in Figure (6), selected in the thermal model. "SOLID70" has a 3-D thermal conduction capability. The nodes has asingle degree of freedom and each element has 8 nodes . The applicable is 3D transient , steady state analysis. In order to include radiation heat transfer, the element "SURF152", Figure(7), was used with extra node option. It simulates radiation heat loss to a space node and is applicable to 3-D thermal analyses.
 One of the two classes of radiation systems must be specified in ANSYS, either open radiation system or closed one. In case of an open radiation system (in contrast with closed radiation system), in which no surfaces that receive the radiated energy can be specified, a space node should be defined. Space node serves to absorb all radiated energy (ANSYS v.10). Space node temperature was used same as the ambient temperature. Element type "*SURF152*" was used to simulate

radiation and convection heat loss, where it was overlaid on the free faces of element "*SOLID70*".
The peak temperature obtained is 1102°C as shown in figure 8 , The material properties as shown in table (3).

3.3 Tensile Test

To investigate the effect of different welding parameters on tensile strength of welded joint, tensile tests have been conducted using specimen for each of the welded joints. Tensile specimens were machined from the welds according to the ASTM sub-size specimen geometry shown in figure (9), such that the weld nugget was positioned in the middle of the specimen gage length (transverse specimen).
The test results have been compared with the base metal .The competence for friction stir welding have been calculated for each experiment as follows:.
Joint Efficiency = test of tensile strength / ultimate tensile strength (Base metal).
        Frome the results noticed that the mechanical properties affected by welding parameters (rotational speed and welding speed) for welded plates.
On my view to obtain high quality of (FSW) welded joints with high mechanical properties i.e. high welding efficiency; the main welding parameters(rotational speed, welding speed) must be carefully selected to obtain high efficiency as shown in table (3), the tensile tests strength and its efficiency are decreased directly with increasing of welding speed.
In this work the selscted metal gives high welding efficiency when welded using (700 RPM rotational speed, 25 mm/min welding speed) that get (100.02%) welding joint efficiency.There is afirst time that we obtain the efficiency reach to 100.02 % to weld steel by FSW. Frome Figure (19-12) which explain the relation between the welding speed of welding tool and tensile strength for the same rotational speed ,as welding speed increase(more than 25 mm/min) the tensile strength decrease for the same rotational speed due to decrease in heat generation.

3.4 Corrosion Resistance Test.

The current and potential had passed (-309.4 mV) and (565.91 nA/cm²)   are respectively.The experiment had required to15 minutes.The electrochemical cell show that the penetration loss for welded plate are less than the base metal see table 5 .So The corrosion resistance of base metal is lees than stirzone. There are two reasons to interpret these results. Firstly, because there is a change in microstructure and the grain size of stir zone is finer than that of base metal. Secondly, the temperature of friction stir welding is less than the melting point so this degree make a heat treatment (stress releave) to the welded plate . The results that appear in the form of a curves in the computer as shown in figure (13) and figure (14) .

3.5 Microhardness Results

The microhardness was measured from center of welding to the base metal at a spacing of (1mm). Microhardness results show that an increase in hardness values in the stir zone . The increased values are probably because of to the dislocation density of the weld nugget . Another reason to increase the hardness because of the small grain size of perllite phases in the stir zone. For each set of measurement (see Table 6) the micrhardness is decreased with increasing the welding speed because the peak temperature decreased with welding speed increasing. Hardness profiles for each welded samples are shown in Figs.(15-22).

3.6 Microstructure Results

The effect of friction stir welding on the material combines heat flow and plastic strain.The heat generated by friction between the tool shoulder and the top of the sheets, and plastic flow by the rotation of the pin tool. These thermo-mechanical condition vary through the joint. The weld region displayed several microstructurally distinct regions including the stir zone(nugget zone),(along the weld   centerline),a   grain-coarsened   region (surroundingthe stir zone), a grain-refined region (encompassing the grain-coarsened region). The figures (23,24 and 25) show that there is no change in the phases. In other words the nugget zone and

base metal have the same phase(pearlite+ferrite) ,But the difference is in the grains size ,shapes and distribution which gives the difference in mechanical properties.The pearlite has yarn shape with homogeneous distribution in the base metal ,while it has different sizes   masses and nonhomogeneouse distribution in nugget zone. In heat affected zone the particales of pearlite as form homogeneouse masess

CONCLUSIONS

According to results of the present study of (FSW) process   on   selected   steel,   several conclusions can be   writing regarding alloy weldability,mechanical,   microstructural   and modeling .
- Low alloy steel with (0.13%C) is weldable using different (FSW) paramrters giving different welding efficiencies.
- The maximum weld strength obtained in this   study   was   (437.09   MPa)   or (100.02%)weld efficiency with (14.20 %) elongation is recorded in the weld.
- The   weld   region   displayed   several microstructurally distinct regions, But there is no change in the phases, In other words the nugget zone and base metal have the same   phase(pearlite+ferrite)   ,But   the difference is in the grains size ,shapes and distribution.
- FSW defects are related to welding parameters , defect free (FSW) welds can be obtained using best main welding parameters(700 RPM + 25mm/min).
- FSW for steel gives a very good corrosion resistance with respect to the base metal.
- The   peak   temperature   theoretically obtained was 1102°C, which was less than the melting point of low carbon steel.

REFERENCES

ANSYS v.10 help, "ANSYS Theory reference".

Hwanga ,Yeong-Haw Hawang,Zong –Wei kang,yuang-cherng chiou and Hung Hsion Hsu, 2008. "Experimental Study on Temperature Distributions within the Workpiece during Friction Stir Welding of Aluminum Alloys." International Journal of Machine Tools and Manufacture, No. 48, pp 778–787.

John A. Goldak and 2005 Mehdi Akhlaghi, "Computation Welding Mechanics" Springer Science and Business Media, Inc.

Naiyi Li,Tsung-Yu,Ronald P. Cooper,Dan Q. Houston,Zhili Feng and Michael L. Santella. 2004. FRICTION STIR

Thomas WM, Nicholas ED, Needham JC, Church MG, Templesmith P., Dawes C. Intl. 1991 Patent Application no PCT/GB92/02203 and GB Patent Application no. 9125978.9,.

T. Saeid ,A. Abdoollah zadeh ,H.Assadi and F. Malek Ghaini. 2008 Effect of friction stir welding speed on the microstructure and mechanical properties of a duplex stainless steel , Materials Science and Engineering A 496 pp 262–268

WELDING OF MAGNESIUM AM60 ALLOY. Magnesium Technology Edited by A. Lou

Scott M. Packer ,Tracy W. Nelson,Russell J. Steel and Murray Mahoney.2005. Tool Geometries and Process Parameters Required to Friction Stir Weld High Melting Temperature Materials

Takehiko Watanabe ,Hirofumi Takayama and Atsushi Yanagisawa 2006" Joining of aluminum alloy to steel by friction stir welding" Journal of Materials Processing Technology 178 pp. 342–349.

Terry Dickerson ,Qing-yu Shi and Hugh Shercliff.2003. HEAT FLOW INTO FRICTION STIR WELDING TOOLS , 4th International Symposium on Friction Stir Welding.

X.K. Zhu, Y.J. Chao 2004. Numerical simulation of transient temperature and residual stresses in friction stir welding of 304L stainless steel 146 pp 263–272

Y.S. Sato ,H. Kokawa and T. Furuhara. 2007. Microstructural evolution of ultrahigh carbon steel during friction stir welding 57 pp 557–560

NOMENCLATURE

A	:	Cross section area of the tool (mm2)
Cp	:	The specific heat (J/Kg.K)
Ff	:	Friction force (N).
Fn	:	Normal force (N).
k	:	Heat conductivity (W/m.k)
T	:	Temperature (K or °C).
FSW	:	Friction stir welding

Greek Symbols

υ	:	Welding speed (mm/min).
ω	:	Rotational speed (rev/min)
ρ	:	Density (Kg/m3).
μ	:	Coefficient of friction.

Fig. 1 Welding Tool
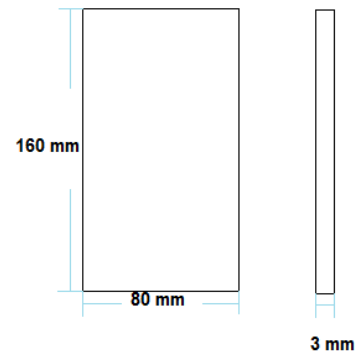
Fig. 2 welding plate

Table 1 Details of the tool used in friction stir welding.

Tool Feature		Tool Detaile
Shoulder	Diameter	16 mm
	Material	WC
Probe	Base Diameter	4mm
	Top Diameter	2mm
	Length	2.6mm
	Material	WC

Table (2): The chemical composition of Plates A516 ASTM.

Sample	C %	Si%	Mn%	P%	S%	Cr%	Mo%	Ni%	Cu%	Al%	Fe%
Chemical composition	0.130	0.003	0.496	0.008	0.003	0.007	0.002	0.042	0.036	0.040	Bal.

Fig. 3 a groove-like defect
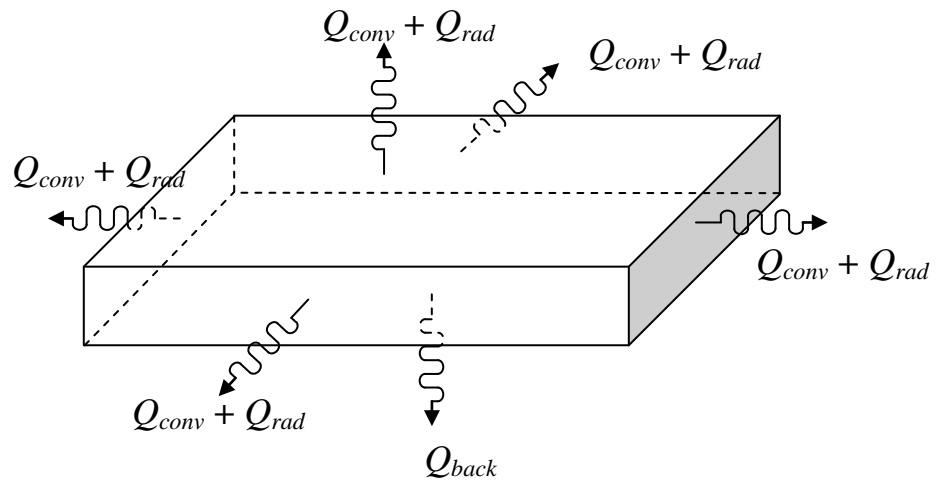
Fig.4 Thermal Boundary Conditions.

*Global
Y- axis*

**Local – Moving
Coordinate**

$X_{i+1} = X_i + V_t \, \Delta t$

*Global
X- axis*

*Initial
position*   *i*   *i+1*   *i+2*   *Final
position*
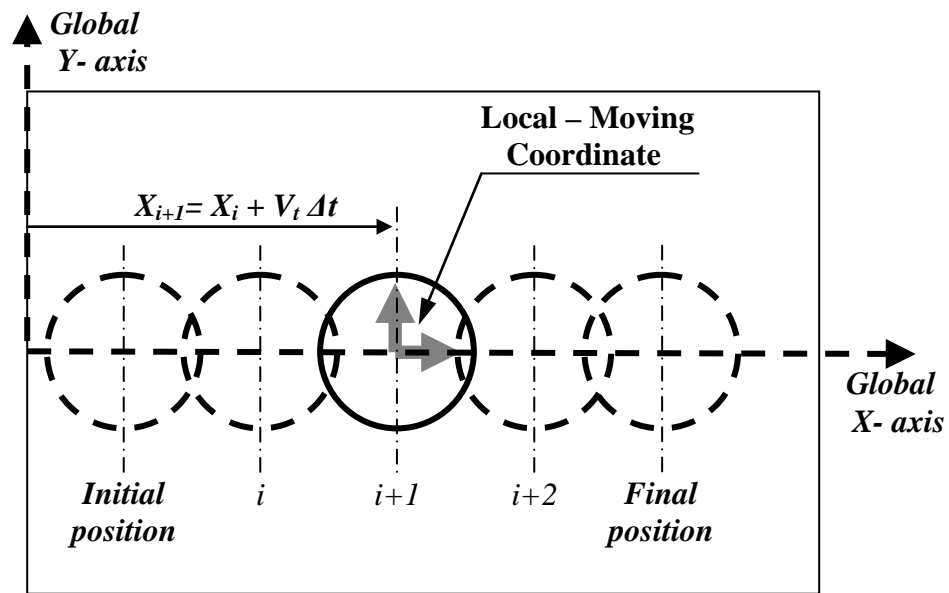
Fig. 5 Modeling of Heat Source Movement at Different Time
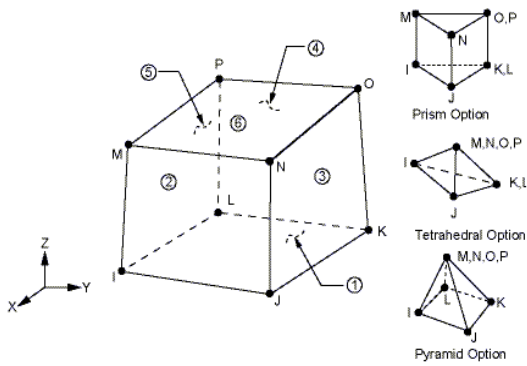
**Fig. 6 Geometry of Element
 "*SOLID70*" (ANSYS v.10)**
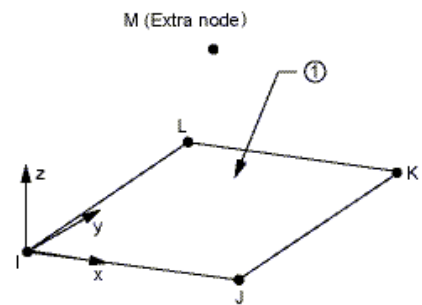
**Fig. 7 Geometry of Element
"*SURF152*" (ANSYS v.10)**

Table 3 material properties for low carbon steel

Sl. No	Temperature (°C)	Thermal conductivity (W/m°C)	Specific heat (J/Kg° C)
1	0	16	500
2	200	19	540
3	400	21	560
4	600	24	590
5	800	29	600
6	1000	30	610
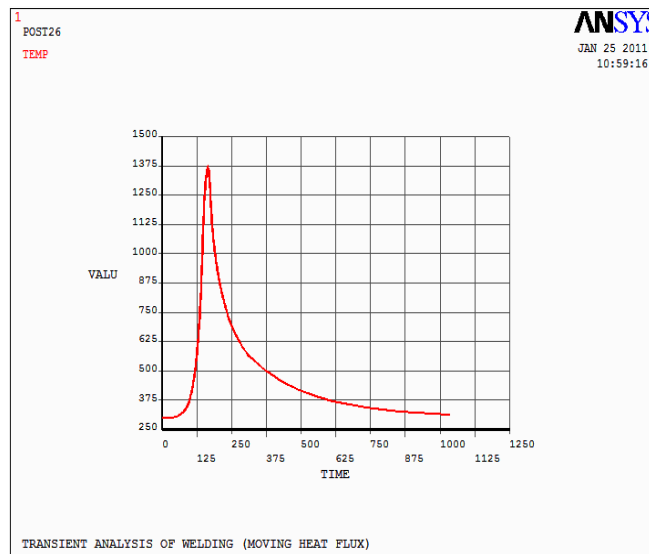
Fig.8 maximum temp. (K°) in center of welded line at(700 RPM+25 mm/min)
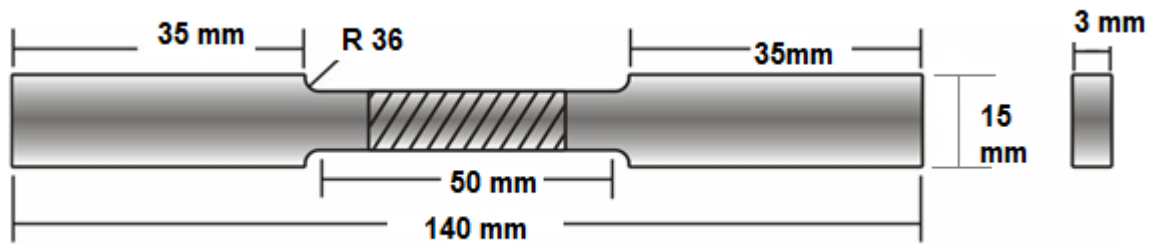
Fig.9 ASTM (E8) Sample for Tensile Test .

Table 4 Tensile test results

	Fsw Exp.	Rotational speed (RPM)	Welding speed (mm/min)	Tensile strength (N/mm²)	Elongation(%)	Joint efficiency in terms of tensile strength (%)
	Base metal	-	-	427.29	14.75	-
Set 1	FSW1	450	25	354.64	3.55	82.99
	FSW2	450	50	141.54	1.43	33.12
	FSW3	450	150	Fail	Fail	Fail
Set 2	FSW4	700	25	437.09	14.20	100.02
	FSW5	700	50	397.00	4,29	92.29
	FSW6	700	150	220	2.06	51.48
Set 3	FSW7	900	25	384.72	4.95	90.03
	FSW8	900	50	325.56	5.03	76.19
	FSW9	900	150	267.44	2.24	62.58
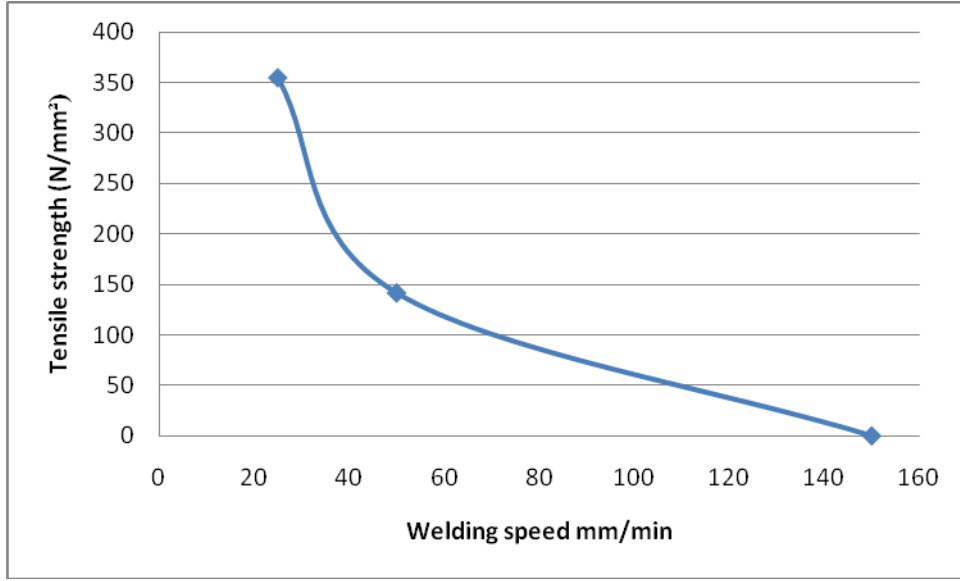
Fig. 10 Relation between welding speed and tensile strength at 450 rpm.
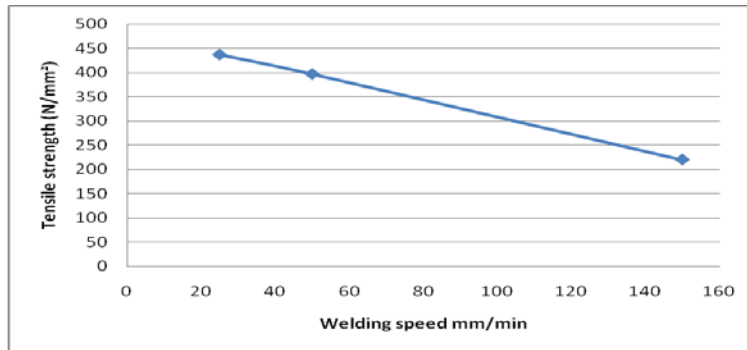
Fig. 11 Relation between welding speed and tensile strength at 700rpm.
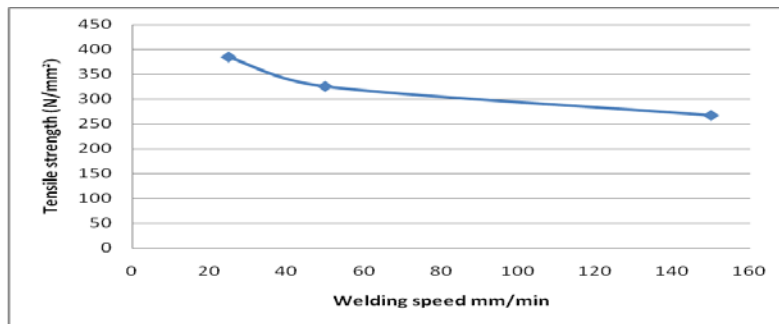
Figure 12 Relation between welding speed and tensile strength at 900rpm.

143

Table 5 Results of corrosion tests

Exp. NO.	Weight loss (g/m² *d)
Base metal	4.07E.001
Welded plate	1.41E.001

Table 6 Results of Microhardness test for FSW Joints

FSW NO.		Microhardness in the center welding (HVN)
BASE METAL		183
Set 1	**FSW1**	255
	FSW2	224
	FSW3	FAIL
Set 2	**FSW4**	276
	FSW5	210
	FSW6	172
Set 3	**FSW7**	291
	FSW8	280
	FSW9	258

144
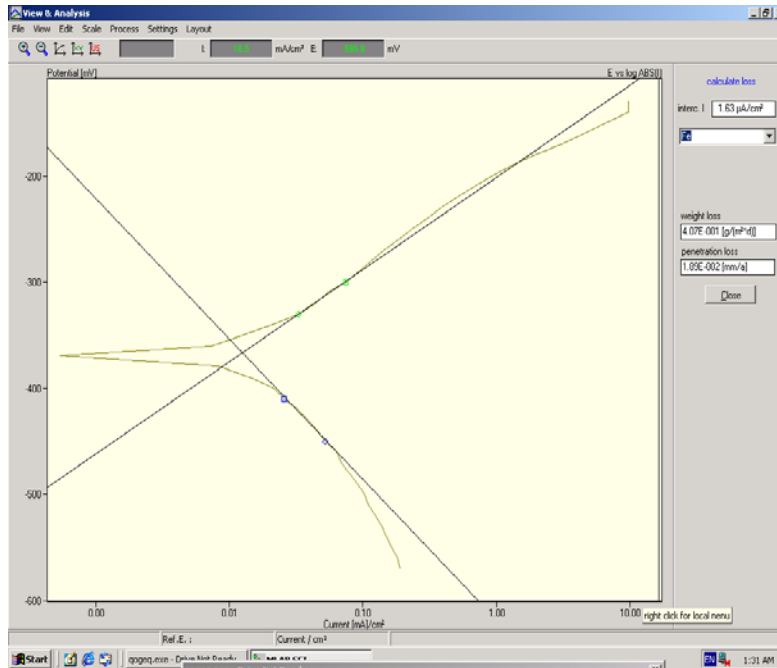
Fig. 13 current-potential curve for base metal.
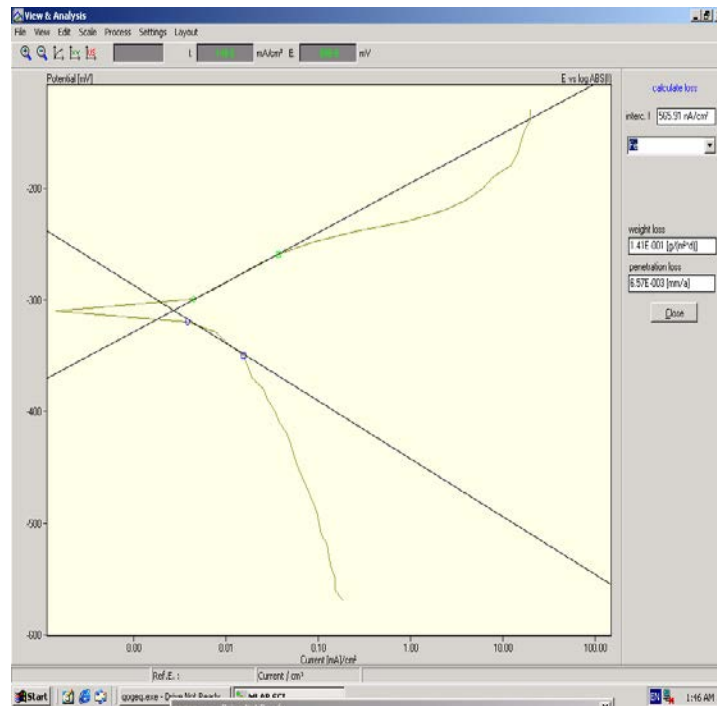
Fig.14 current-potential curve for welded region.
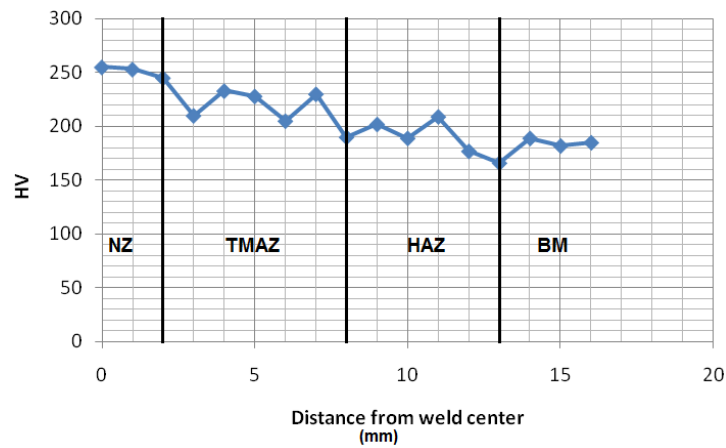
Fig.15 Microhardness Profile in FSW1
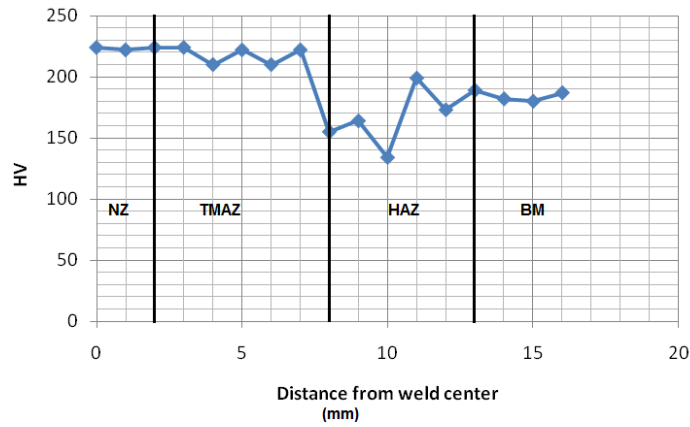
Fig.16 Microhardness Profile in FSW2
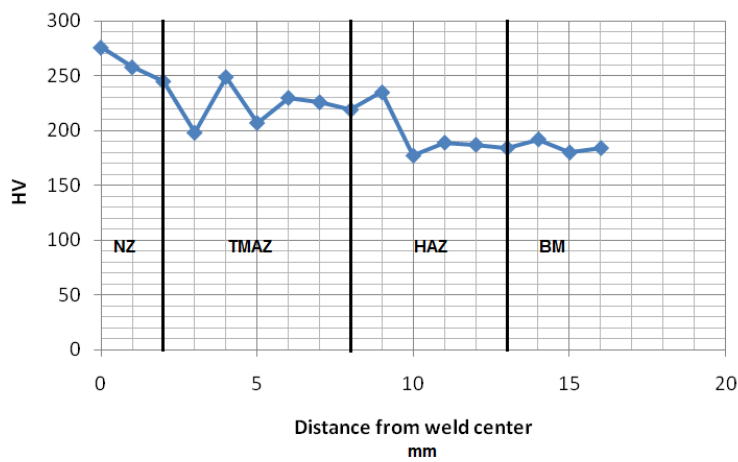
Fig.17 Microhardness Profile in FSW4
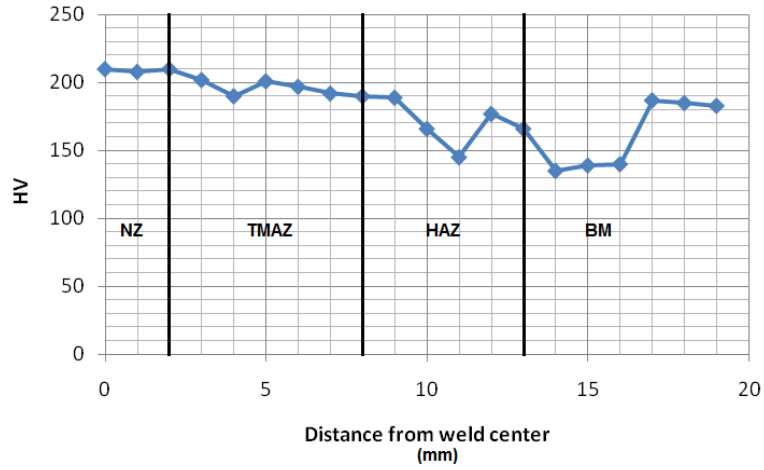
Fig.18 Microhardness Profile in FSW5
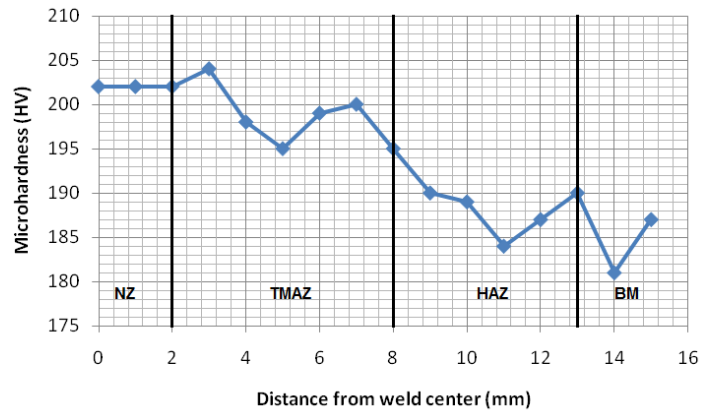
Fig.19 Microhardness Profile in FSW6
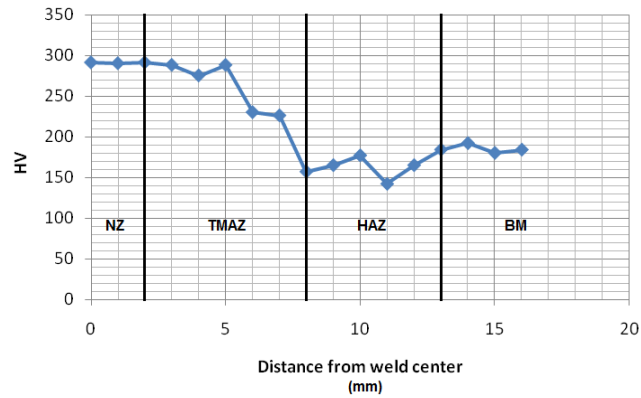
Fig.20 Microhardness Profile in FSW7

Fig.21 Microhardness Profile in FSW8
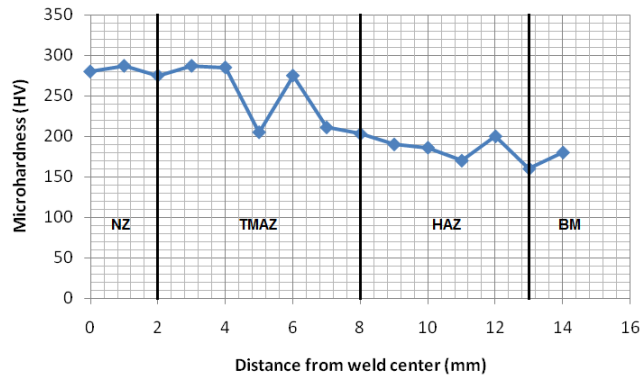
Fig.22 Microhardness Profile in FSW9

Pearlite

Ferrite
(matrix)
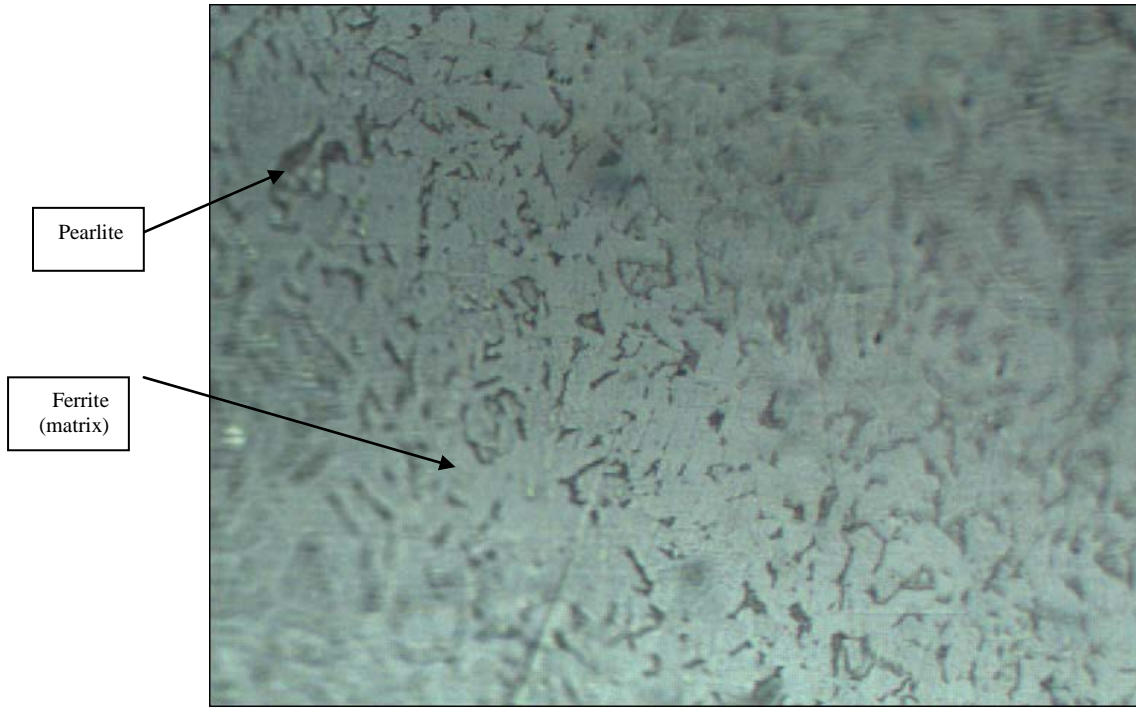
Fig. 23 Base metal structure (X40)
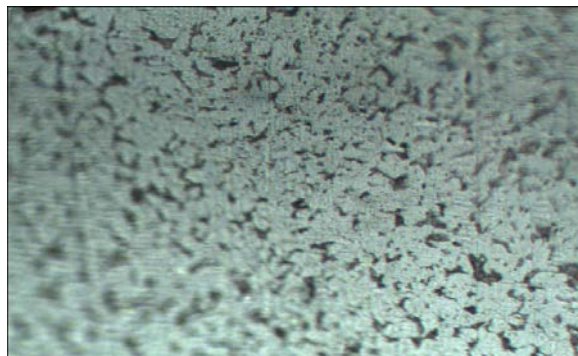
Fig. 24 Nugget structure zone. (X40)
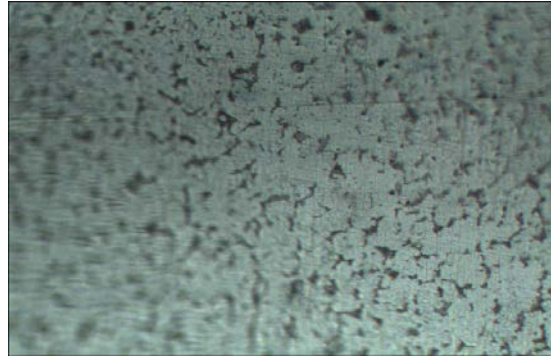
Fig. 25 Heat effected structure zone. (X40)

(a) FSW4   (b) FSW5   (c) FSW7   (d) FSW1   (e) FSW8

(f) FSW9   **(g)** FSW6   **(h)** FSW2   **(i)** FSW3

Fig 26 Welding plates